

## EXPERIMENTAL INVESTIGATIONS OF A VERY LONG RANGE INFRASONIC ANNULAR SYNTHETIC-JET

V. Tesař\*, K. Peszyński\*\*

**Summary:** Authors investigated an annular synthetic jet required to reach to very large distances while operated at infrasonic frequency. Hot-wire measurements of velocity profiles indicate the range to be roughly 4-times the distance achievable with the steady jet generated in the same nozzle.

### 1. Introduction

The motivation for the study of the investigated annular synthetic jet was its potential application in walk-through portal detectors for anti-terrorist warfare (Tesař 2007, Tesař and Peszynski 2009). The jet is intended to form a protective cylindrical boundary surrounding

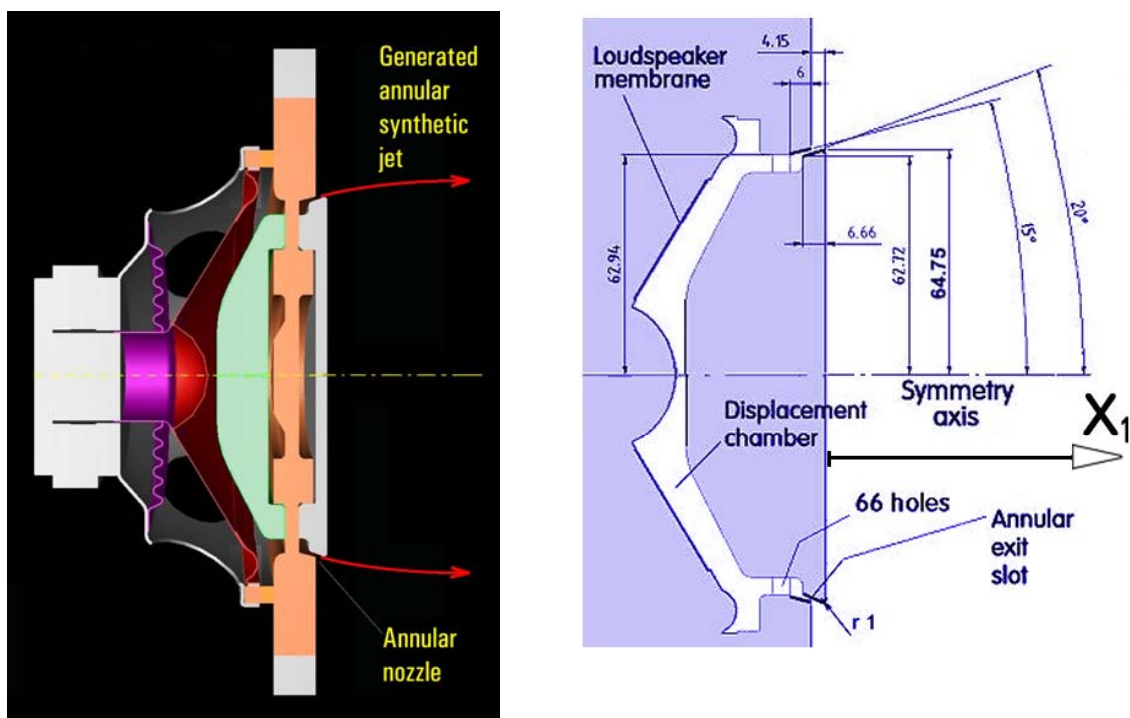


Figure 1 (Left) The layout of the actuator designed to generate the annular synthetic jet reaching to very large distances. Note the lips of the annular nozzle directed outwards.

Figure 2 (Right) Geometry of the actuator used in the present investigations .

\* Prof. Ing. Václav Tesař, CSc., Institute of Thermomechanics, Academy of Sciences of the Czech Republic v.v.i.; Dolejšková 5, 182 00 Praha 8; Czech Republic, tel.: +420 2 6605 2270, e-mail: [tesar@it.cas.cz](mailto:tesar@it.cas.cz)

\*\* Doc. Ing. Kazimierz Peszynski, CSc., Department of Control and Machinery Design, University of Technology and Life Sciences, ul. Prof. S. Kaliskiego 7, 85-789 Bydgoszcz, phone +48 52 340 8238, fax + 48 52 340 82 45, e-mail: [kazimierz.peszynski@mail.utp.edu.pl](mailto:kazimierz.peszynski@mail.utp.edu.pl)

the space between the detector at the one end and - at the other end - the surface of the person's clothing tested for presence of an illegal material (explosives or drugs). The jet prevents mixing of the air in this space with the outer atmospheric air. Since the illicit material is present only in trace amounts, avoidance of its further dilution by external air is of paramount importance and this is what the annular jet does. To use for this protection task a synthetic jet – generated by alternating outflow and inflow through the nozzle - was proposed by Tesař and Trávníček in 2006 and discussed by Tesař, Vogel, and Trávníček (2008). The synthetic jet is produced in an actuator nozzle by means of the aerodynamic rectification phenomenon (Tesař 1982, 2008), originally investigated by the present principal author for uses in fluidics (Tesař 1976, 1980, 1981a, 1981b, 1982, 1984, 1991, 1996), a long time before it was given, by Prof. Glezer, the name under which it is currently known.

Most applications of synthetic jets are in control of fluid flow past bodies (Tesař 2006), usually by generation of streamwise vortices (Tesař, Kordík, and Daněk, 2008). This calls for a rather high operating frequency, of the order of 0.1 kHz. In the present application, however, the operation in the audible frequency range would cause inconvenience. The basic requirement therefore was placed on operations at an infrasonic (Gavreau, 1968), inaudible frequency less than or at most equal to 20 Hz.

## 2. The problem of the long range

The detection of substances removed from persons' clothing is, of course, complicated by the vast existing anthropometric differences between individual persons passing through the detection portal — in the inner walls of which the actuator is positioned. Variations in human body breadth, measured as the standard deviation, is about 25 % of the mean (Ruff, 2002). Statistical data indicate that 5 % of men living in the USA have shoulder breadth more than 510 mm while, at the other extreme of the spectrum, only 5 % of Hong Kong women have their shoulder breadth less than 355 mm. This means that to accommodate 90 % of all persons

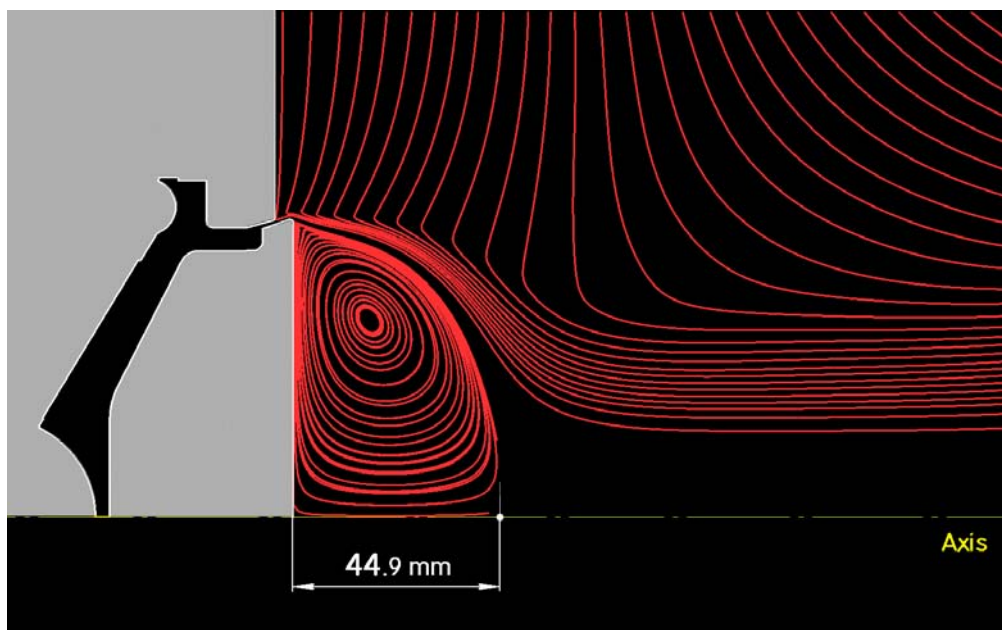


Figure 3 Pathlines computed by numerical flowfield solution of the steady annular jet generated in the same nozzle (Fig. 2) as the one used in the synthetic-jet experiments.

likely to be tested (provided, of course, the portal is set up so as to avoid person's evasive movements when passing through), it is sufficient to design the detector so as to be able to cover 155 mm distance variations. This does not mean 155 mm distance from the actuator nozzle since 10 mm has to be added for thickness of indoor clothing (a thicker heavy outdoor clothing may be assumed removed for the test) and an additional safety distance of another 15 mm for avoiding too frequent contact with the portal walls. Usually, there will be at least two detectors in the inner walls of the portal. If placed opposing one another, the required synthetic jet range will be one half of the above 180 mm sum.

Achieving this required 90 mm distance with a steady annular jet would be highly impractical as it would necessitate a very large diameter actuator, leading to high consumption of expensive compressed air. Figure 3 presents an example computed for the 130 mm diameter annular nozzle of the geometry from Fig. 2. The jet entrains outer air on both its inner as well as outer sides – by the effect called jet-pumping. Since on its inner side the entrained and removed air cannot be replaced, a low-pressure region is produced there. This bends the jet towards the axis, finally closing this region in a stagnation point on the axis. In an attempt to counteract this bending of the jet towards the axis, the lips of the nozzle exit in this design are oriented outwards, away from the axis (note the 15° and 20° angles in Fig. 2). The resultant effect, however, is seen in Fig. 3 to be marginal. The result of the jet turning towards the axis is a relatively short bubble formed in front of the nozzle exit, its axial length in Fig. 3 being less than 35 % of the nozzle diameter – or, in other words, just one half of the required 90 mm.

### 3. Experimental investigation of the synthetic jet

Previous experimental evidence with annular synthetic jets, e.g. Tesař & Trávníček 2005, has shown much smaller bending of the jet towards the axis than is the case with steady jets. This is beneficial for the detector design. For verification of the idea that the resultant range of the

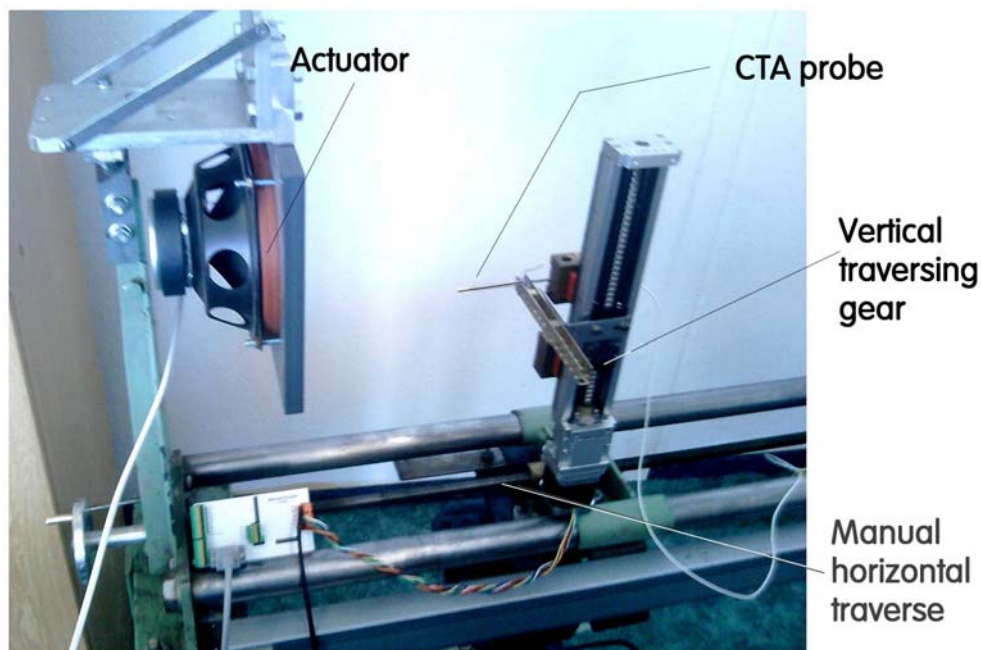


Figure 4 Photograph of the experimental setup. The model actuator is at left, at right is the hot-wire anemometer probe moved in the meridian plane by the two mutually orthogonal traversing gears, the vertical one controlled directly by the data acquisition computer.

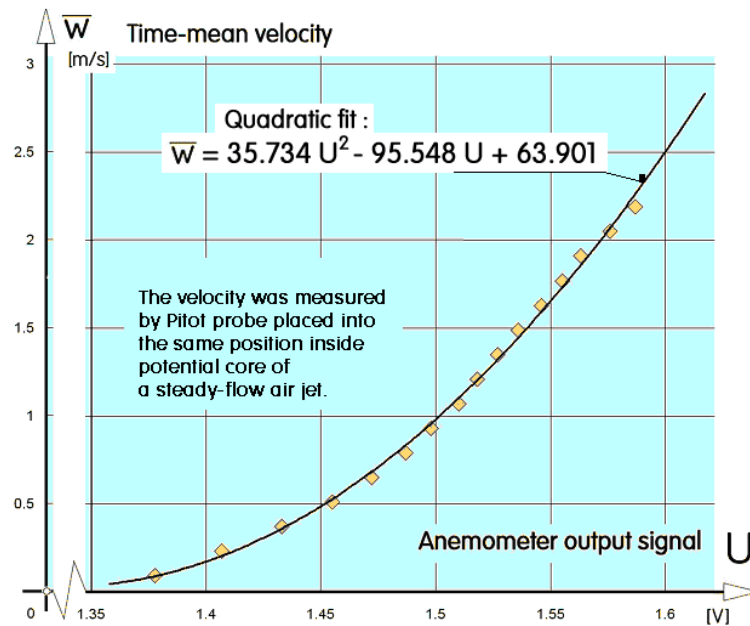


Figure 5 The calibration curve of the hot-wire probe. The calibration was performed, prior to the actual test runs, with special attention paid to the range of low velocities.

protected space (inside the jet annulus) will be longer with the synthetic jet, a model of the actuator (as shown in Fig. 1) was built and investigated in laboratory. Nominal diameter of the nozzle is 130 mm and the width of the nozzle slot (again nominal, because the shape of the nozzle exit does not permit an unequivocal width definition) is  $b = 1$  mm. The alternating displacement motion for the jet generation was produced by a commercially available woofer loudspeaker ARN-165-01/4. Apart of the inclination of the nozzle lips, it may be noted in Figs. 1 and 2 that to counter the trend to the formation of a closed-flow short bubble in front of the nozzle, the issuing jet was directed slightly into the outward direction (away from the nozzle axis) also by the 4.15 mm stagger of the nozzle exit lips - the internal nozzle lip is longer by this distance than the outer one.

In pulsating flow through orifices (Tesař, 1989), the efficiency of generating the alternating output flow may be significantly decreased by the capacitance of the cavities (Tesař 2007, Tesař & Peszynski 2005) located upstream from the exit. Instead of moving air out through the nozzle to form the jet, the moving membrane may just compress and expand the air inside the cavities (Tesař, Trávníček, Kordík, Broučková, 2009). To decrease this effect, the volume inside the conical membrane of the loudspeaker was made smaller by the inserted solid centrebody (shown in green colour in Fig. 1).

The laboratory measurements, performed in the setup shown in Fig. 4, concentrated on measuring air flow velocity in the generated synthetic jet. The used instrumentation was the hot-wire anemometer system CTA 54T30 (DANTEC Dynamics) with standard single-wire probe type 55P16. The probe was traversed in the radial direction by an automatic traversing gear (Fig. 4), driven by a stepping motor. At each location the probe remained stationary for the duration of the data acquisition. The computer control of the traversing, as well as an elegant method of data acquisition using the data storage properties of the digital oscilloscope RIGOL DC 1042CD, were devised by our colleague Mr. M. Pavelka. Before the actual experiment, the anemometric system was calibrated (Fig. 5) by comparison with Pitot probe

positioned in parallel with the hot-wire probe in the potential core of the same auxiliary air jet. The parameters of the adjustment, such as the probe currents were as supplied by the probe and anemometer manufacturer.

The heated wire of the anemometer probe was held so that its axis was oriented in the tangential direction relative to the nozzle axis – i. e. the wire was perpendicular to the meridian plane in which it was moved. Of course, the probe was sensitive not only to the axial component of the air flow velocity, but also to the radial component (and insensitive to the tangential velocity component, which in this axisymmetric flow case is negligible anyway). The measured values are therefore in the following text described as velocity magnitudes (or magnitudes of the velocity vector in the meridian plane). This is not of importance in the main part of the jet, on which the attention was focused here, because the axial component was substantially higher there. It may be, however, a partial explanation for the fact that the measured velocity magnitude values never reach the zero value at large radial distances from the jet axis (note the non-zero values in Fig. 6 for  $X_2 > 100$  mm). The other part of the explanation for the non-zero values there is the inability of the hot-wire probe to discriminate between positive and negative direction of the velocity. The large-scale vortices present at the edges of the jet and moving there past the probe may lead to temporary negative axial velocity component value – which is not recognised by the probe and shown as a positive value.

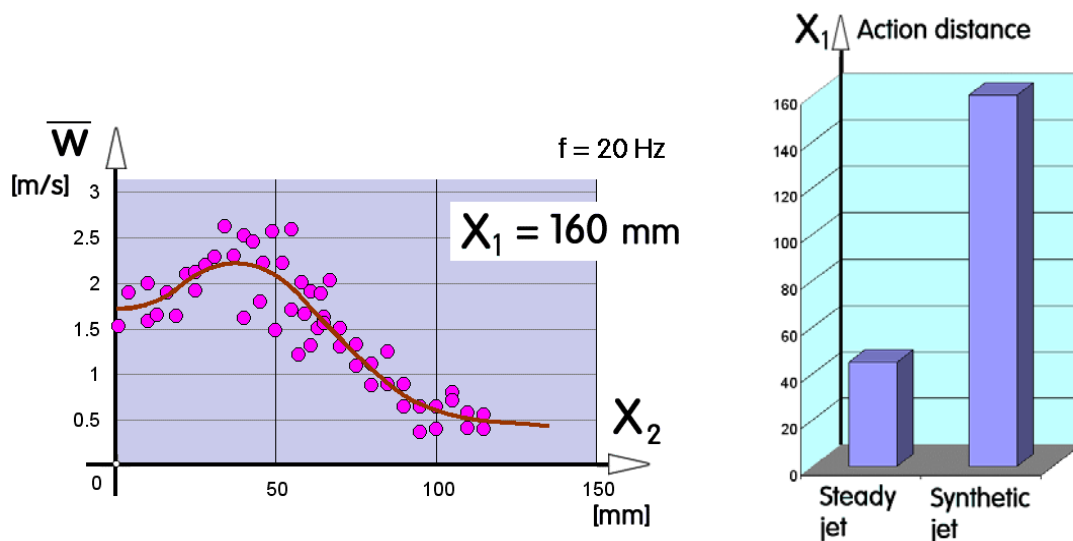


Figure 6 (Left) An example of the recorded values of the time-mean magnitude of the velocity vector in the meridian plane measured at very large axial distances  $X_1$  from the nozzle exit (cf. the definition of  $X_1$  in Fig. 2). The heavy line is a 6-th order polynomial fit.

Figure 7 (Right) The comparison of the range into which the protective effect of the jet extends with the steady-flow jet (Fig. 3) and with the synthetic jet.

The success of the idea of using the synthetic jet for providing an cylindrical protected space reaching into long distances from the nozzle is seen in Figs. 6 and 7. Presented in Fig. 6 is the typical example of the velocity data measured at a very large axial distance from the nozzle,  $X_1 = 160$  mm, i.e. at 123 % of the nominal nozzle diameter. Despite the very large scatter (which was due to the time scale of data acquisition inevitably too short relative to the characteristic time scale of the large vortical motions prevailing there) it is immediately

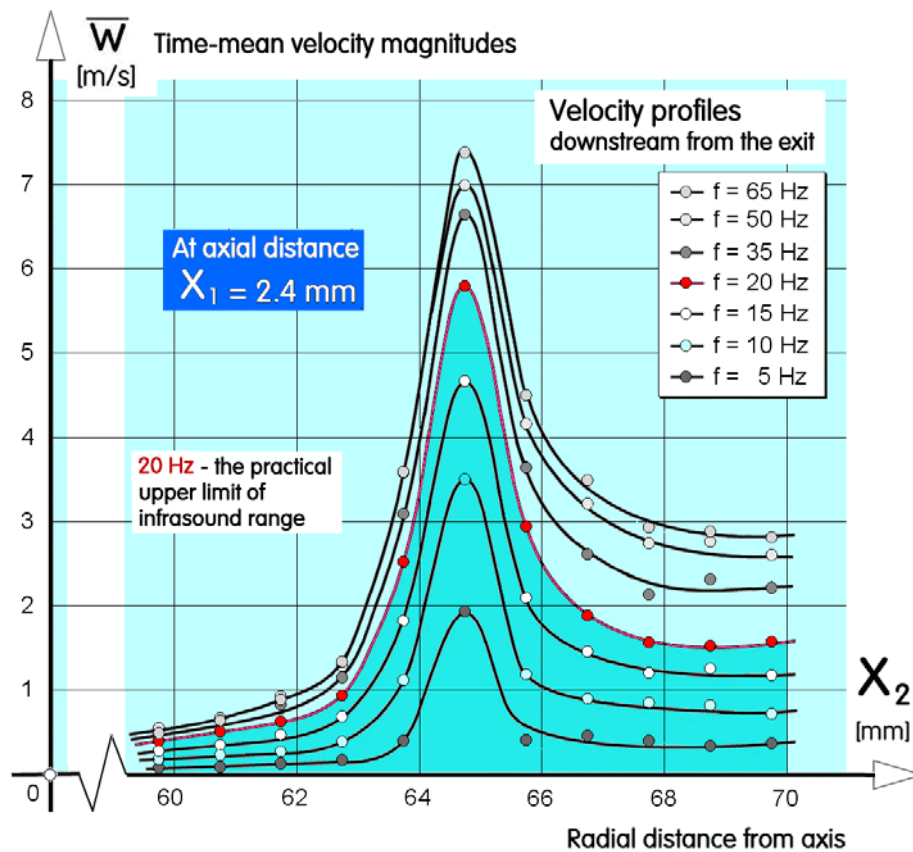


Figure 8 The time-mean velocities near the nozzle exit found by measurements taken at different actuator driving frequency. The infrasound requirement limits the applicability of frequencies  $f \leq 20$  Hz

recognisable that the time-mean flow in the synthetic jet has a different character than what is shown for the same axial distance with the steady annular jet in Fig. 3. The critical feature is the local minimum of the velocity values near the axis, at  $X_2 = 0$  in Fig. 6. The steady jet downstream from the recirculation bubble stagnation point would exhibit at the axis a local maximum (Tesař & Trávníček, 2008). Very probably, the local minimum indicating a different character is present even at larger distances than  $X_1 = 160$  mm, but the strong turbulent scatter indicates the high level of chaos makes the jet there hardly useful and for this reason this distance is considered the end of the range for the purpose of Fig. 7 (the chaotic conditions there, if desired, might be decreased by applying a higher driving power in the actuator). At any rate, the comparison presented in Fig. 7 demonstrates clearly the obvious advantage of the synthetic jet for the discussed protection task.

#### 4. Flowfield details at $f = 20$ Hz

Figure 8 above presents the results of time-mean velocity profile measurements made very near to the nozzle exit. Individual curves correspond to data obtained at different driving frequencies (while keeping all other adjustable quantities the same). The 1 mm resolution was not sufficient for showing the details of the initial profiles, but the overall character of the flowfield is obvious: the local maximum corresponds to the nozzle exit flow while the

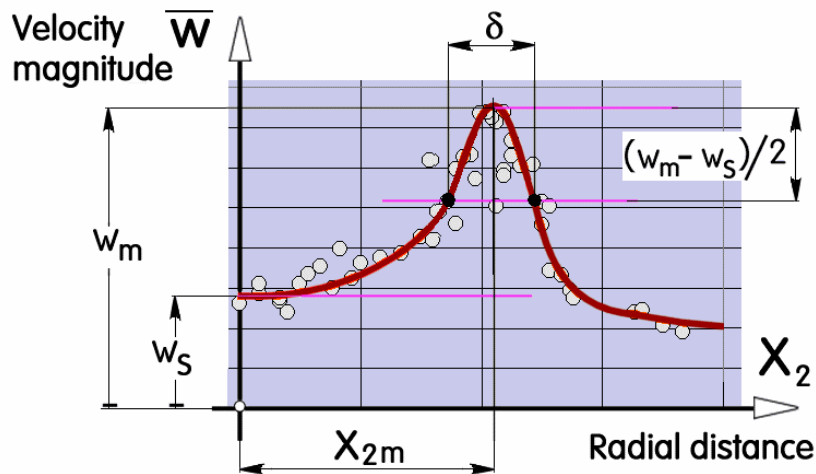


Figure 9 Definition of the geometric quantities evaluated from the experimental velocity profile data. The evaluation proceeded by first fitting a smooth line through the data points and then measuring the various distances in the plotted diagram.

velocities at higher as well as lower  $X_2$  may mainly reflect the radial inflow towards the jet. At the outer side (higher  $X_2$ ) the entrainment into the mixing layer of the forming synthetic jet is more pronounced as it is there easier to get a replacement fluid for one carried away with the jet.

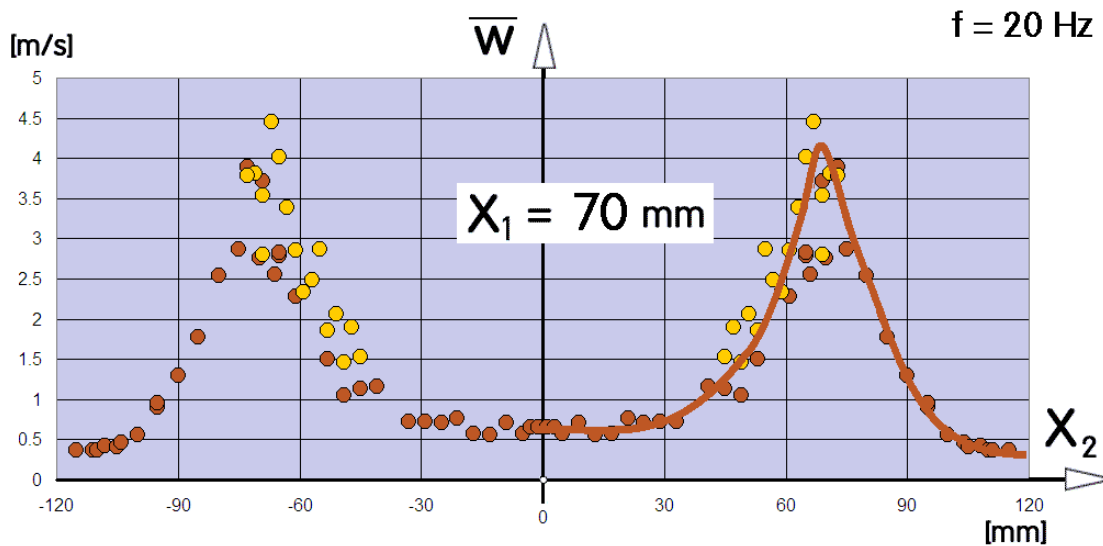


Figure 10 An example of the measured data points (time-mean velocity as a function of radial distance) obtained in two different runs (as indicated by two different colours of the data points) and the fitted smooth line, obtained for the relatively short axial distance  $X_1$  from the nozzle. The two distinct velocity maxima show unequivocally that at this distance there is no closure of a bubble (of the character from Fig. 3).

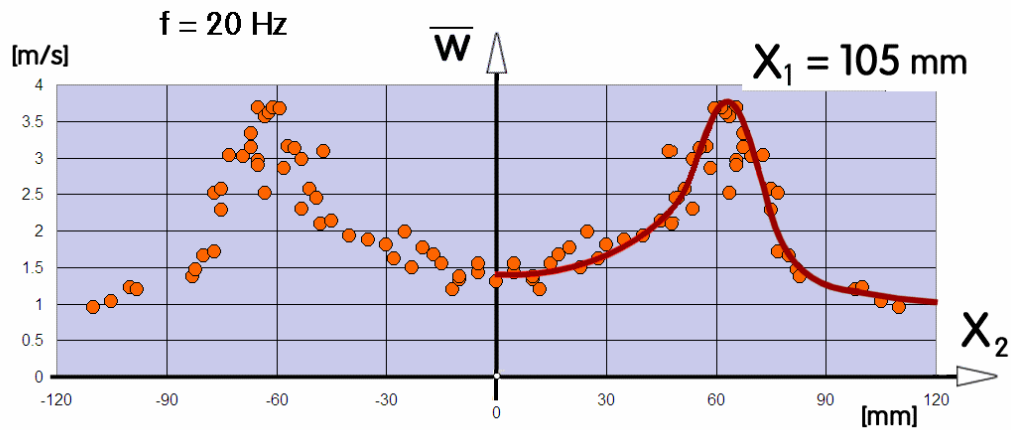


Figure 11 Another typical example of the velocity profile measurements, here at a considerably large distance than in the previous Fig. 12.

The diagram Fig. 8 shows convincingly that the effectiveness of the synthetic jet generation increases in a monotonic manner with the frequency of the applied electric signal. Only because of the demand of the infrasonic operation in the particular application pursued here, as mentioned already in the Introduction, it was necessary to concentrate on the very low frequencies and thus avoid the attractive possibility of working in the more effective regime. All the subsequent measurements were therefore made at what seemed to be top limit of acceptability, the frequency  $f = 20$  Hz.

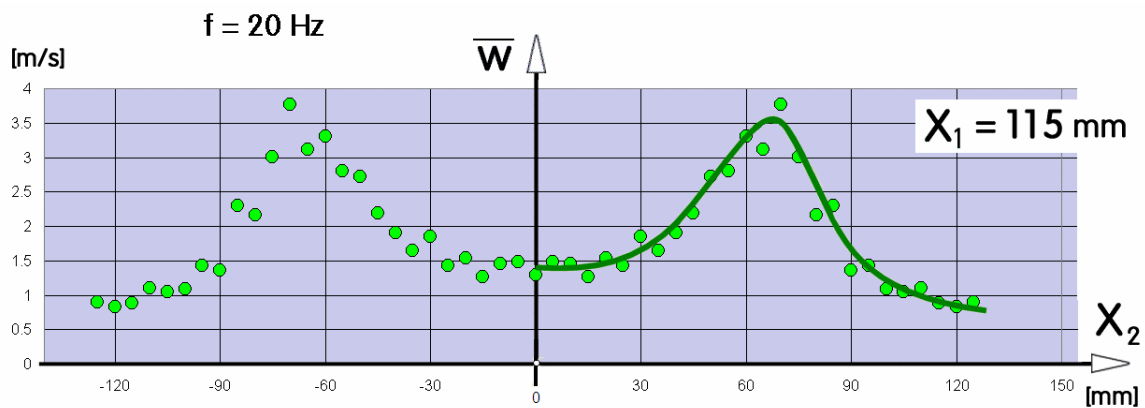


Figure 12 Velocity measurements at the rather large axial distance  $X_1 = 115$  mm.

In contrast to the steady annular jet, which in the streamwise direction changes the topological character of the velocity profiles (Tesař & Trávníček, 2008), in the investigated flow the character remained qualitatively the same. Variations in the axial direction are here only quantitative. For their evaluation in different profiles, a number of quantitative parameters were to be introduced. They are defined in of Fig. 9. To evaluate them, it is first necessary to fit a smoothed line through the data. The line is mostly a polynomial dependence – in some cases with manual corrections at the high  $X_2$  end. The parameters are then measured between characteristic points on this line.



The quantification parameters introduce here are as follows:

- the time-mean velocity maximum  $w_m$  in the peaks of the profile,
- the local minimum time-mean maximum  $w_m$  between the peaks (due to the symmetry of the problem this is located on the jet axis)
- the convention jet width  $\delta$  ( defined as the radial distance between the two points in which the time-mean velocities are equal to one half of the difference between  $w_m$  and  $w_m$  )
- the radial distance  $X_{2m}$  from the jet axis to the velocity maximum.

Examples of the time-mean velocity profiles and the fitted smooth lines are presented in Figs. 10 to 14. The general trends observed in this succession of the profiles are in agreement with what may be expected as a result of the air mass flow rate in subsequent cross sections along the jet increasing by entrainment of the outer air.

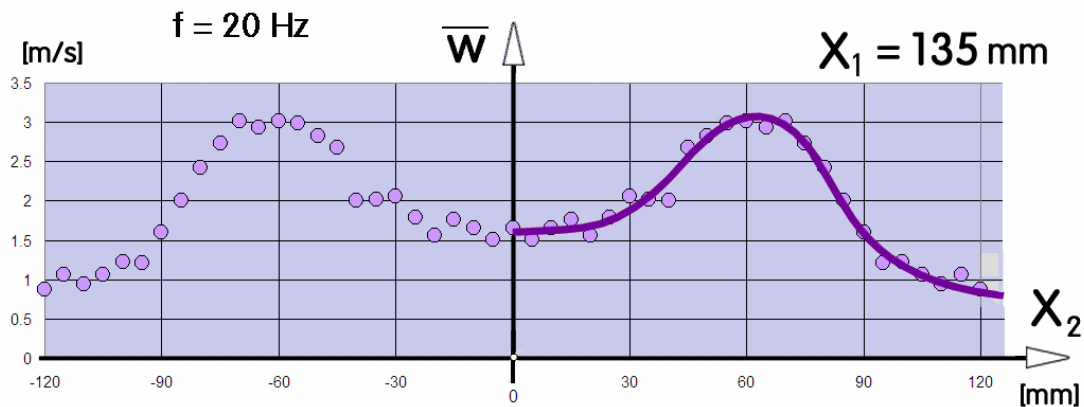


Figure 13 The invariant topological character of the velocity profiles (compared with the previous cases as shown in Figs. 10 to 12) is here demonstrated on the very similar velocity-magnitude profile measured at the axial distance  $X_1 = 135$  mm.

First, the maximum velocity  $w_m$  gradually decreases while the jet width  $\delta$ . This is the necessary consequence of retaining the axial momentum with a larger moving mass. The velocity profile peaks, quite sharp at the beginning, become progressively more flat and wide.

Second, the maxima on the opposite sides of the jet axis gradually approach one another. This, to a certain degree, suggests a trend similar to the closure of the bubble as was shown above in Fig. 3, but the progress in that direction in the synthetic jet is much weaker. As already mentioned in association with Fig. 6, the mechanism is different. The "bubble" – the protected region of interest in the proposed application – is certainly not closed by the appearance on the jet axis of the stagnation point.

Third, what finally limits the applicability of the annular synthetic jet is obviously the gradual filling of the low-velocity minimum at and near the jet axis. This is probably due to some radial transport of axial momentum towards this local minimum.

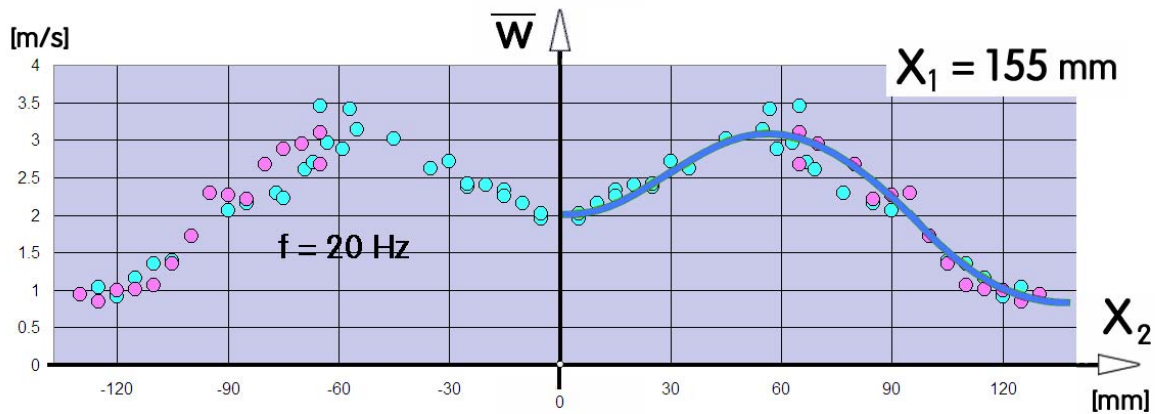


Figure 14 Yet another demonstration of the invariant topology, a velocity profile measured at the very large distance equal to 110 % of the nominal nozzle diameter. Of course, the details of the profile change – the velocity maxima are wider and lower – but the overall character is not changed, demonstrating the lack of any tendency of closing a low-pressure bubble.

### 5. Summary of experimental results.

Numerical values of the quantification parameters evaluated for the individual profiles were then plotted as a function of the axial distance  $X_1$  from the nozzle in the three final diagrams, Figs. 15 to 17. It was found possible to fit straight lines with reasonable accuracy through the data points in all these diagrams. This, however, is not to be interpreted as a demonstration

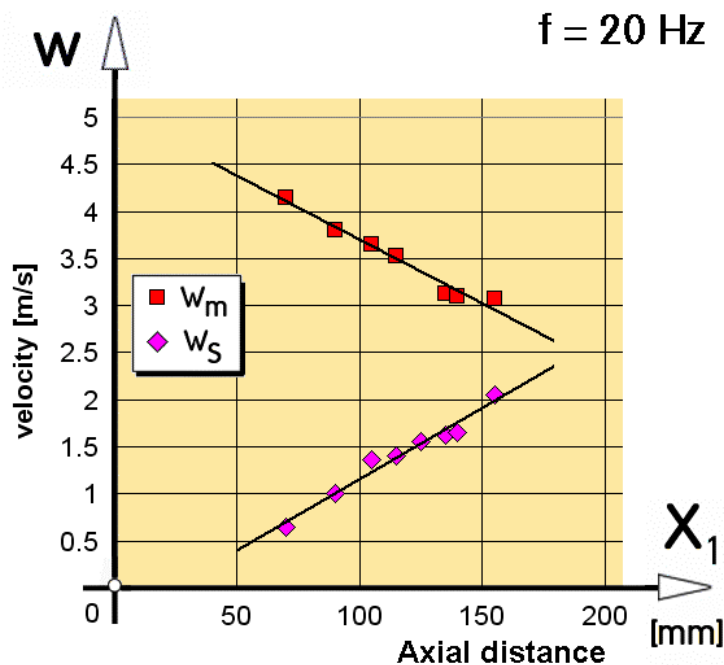


Figure 15 Presentation of the velocity-profile details measured from some of the data shown in Figs. 10 to 14 (as well as some other, not shown here). The velocities defined in Fig. 9 are plotted as a function of the streamwise, axial distance from the nozzle.

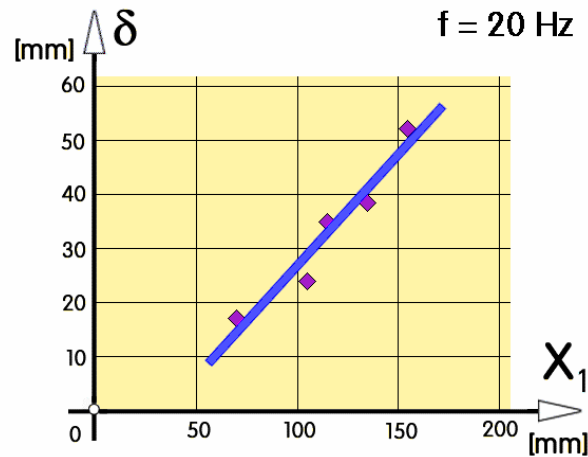


Figure 16 The streamwise changes of the annular nozzle widths obtained by evaluation of the smoothed profiles such as they are shown in Figs. 10 to 14. The data may be well fitted by a straight line which, in this particular case, has some theoretical substantiation.

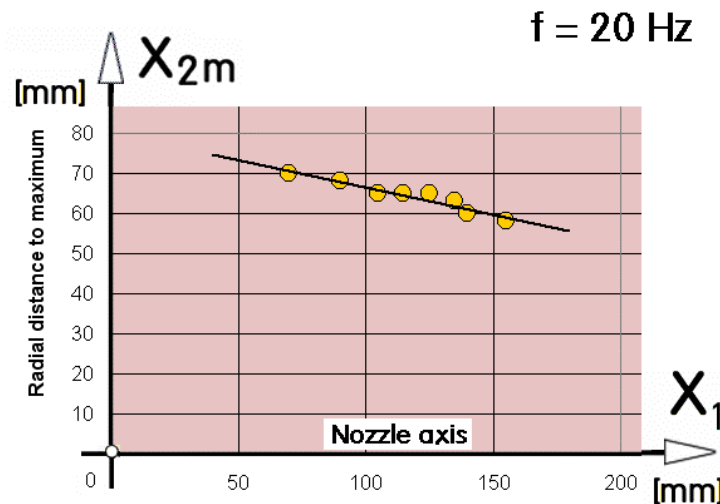


Figure 17 The axial variation of the radial distance from the jet axis to the velocity maximum, in Figs. 10 to 14. The maxima come nearer to one another with the increasing axial distance. The result is a trend similar to the closing of the recirculation bubble of the steady jet (Fig. 3), but the decrease is much slower.

of validity of linear laws of the dependences. In the related investigations of axisymmetric synthetic jets by Tesař & Kordík (2009), the axial variations of the velocity maximum and convention diameter of synthetic jets were found to agree, with reasonable reliability, with the corresponding variations of steady jets. In the present case the interest is focused on the far-field behaviour – near the end of the protected central region – and, as a result, velocity profiles were not studied in detail at the short distances  $X_1$  where the relatively very thin jets may behave as their planar steady-flow counterpart (unless they are influenced by the rather strong difference between the outer and inner side, as it is seen in Fig. 8). In the steady planar jet the velocity maximum, of course, is known to decrease in inverse proportion with the axial distance (measured from the virtual origin). At least the seemingly linear decrease of  $w_m$  with

distance  $X_1$ , however rather attractively suggested in Fig. 15, may be thus a fortuitous results of too short range of the data points and stochastic scatter.

On the other hand, the linear growth of the width with the distance  $X_1$  in Fig. 16, though less convincing due to a higher scatter, may be actually a correct result in view of the linear growth law for turbulent planar jets.

The linear fit in Fig. 17 is just a simplification at any rate, since the origin of the fitted linear dependence does not pass through the radial distance of the exit slot.

## 6. Conclusions

To conclude, it should be said that we have successfully demonstrated generation of an infrasonic annular synthetic jet of the size directly applicable to an important task in the anti-terrorist warfare. Because of the interest focusing on the achievement of the long range, the measurements were made with only single-wire anemometric probe, with the measured data values processed only so as to obtain time-mean velocity data, adequate for the task. The data exhibit rather high scatter, but their fitting by smooth lines seems to be quite convincing.

The most important among the results is the discovered fact that – contrary to the steady annular jet – no recirculation bubble is formed ending in a stagnation point on the jet axis. The end of the usable region is determined by the phenomenon of filling the local velocity minimum so that the velocity dependences on distance  $X_1$  tend (Fig. 15) to mutually intersect.

## 7. Acknowledgement

The authors acknowledge gratefully the support by the grant IAA200760705 from the Grant Agency of the Academy of Sciences of the Czech Republic, and by the grant 101/07/1499 from the Grant Agency of the Czech Republic. The hot wire probe traversing as well as an elegant method of data acquisition were devised by Mr. M. Pavelka.

## REFERENCES

- Gavreau V. (1968), Infrasound, *Science Journal*, Vol. 4, Issue 4, p. 33
- Ruff C. (2002) Variation in Human Body Size and Shape, *Annual Review of Anthropology*, Vol. 31, p. 211
- Tesař V. (1976) Čerpadlo nebo dmychadlo, zejména pro dopravu obtížně čerpatelných tekutin (Pump or blower, in particular for transporting fluids difficult to pump - in Czech), *Czechoslovak Certificate of Authorship* Nr. 192 082
- Tesař V. (1980) Aktivní fluidický uzavírací ventil, (Active Fluidic Turn-Down Valve - in Czech), *Czechoslovak Certificate of Authorship* Nr. 212 802
- Tesař V. (1981a) Fluidic pump driven by alternating air flow, *Proc. Colloquium on Pneumatics and Hydraulics PNEU-HIDRO '81*, Győr, Hungary, p.57
- Tesař V. (1981b) Zařízení k odstraňování prachu z nosiče záznamu, zejména při reprodukci z gramofonové desky (Facility for removal of dust from recoding medium, in particular during a reproduction from gramophone record – in Czech), *Czechoslovak Certificate of Authorship* Nr. 238 658
- Tesař V. (1982) Fluidic jet-type rectifier: experimental study of generated output pressure, *Fluidics Quarterly*, Ann Arbor U.S.A., Vol. 14, Nr. 4

- Tesař V. (1984) Zákonitost pro strhávání okolní tekutiny při střídavém vtoku a výtoku tryskou (Law governing entrainment of surrounding fluid during alternating inflow into and outflow from an orifice - in Czech), PO 86-84, Czechoslovak Patent Office, Prague, Czech Republic
- Tesař V. (1989), Ztráty při pulsujícím výtoku z trysky (Hydraulic Loss of a Nozzle Supplied with Pulsating Flow – in Czech), *Proc. of Conf. 'Aplikácia experimentálnych metód ...'*, p. 23, Tatranske Matliare, Slovakia
- Tesař V. (1991) Strhávací účinek střídavého vtoku a výtoku tryskou (Etrainment action of an alternating inflow into and outflow from a nozzle - in Czech), *Acta Polytechnica*, 1, (II,1), p. 43
- Tesař V. (1996) Fázové trajektorie pulsujícího výtoku vzduchu tryskou (Phase Trajectories of a Pulsating Flow through a Nozzle – in Czech), *Proc. of Colloq. "Dynamika tekutin '96"*, publ. by Institute of Thermomechanics AS ČR, ISBN: 80-85918-23-4, p. 61
- Tesař V. (2006) Fluidics Applied to Flow Control by Synthetic Jets, *Proc. of the Conference "Topical problems of Fluid Mechanics 2006"*, p. 171, ISBN 80-85918-98-6, publ. by Institute of Thermomechanics AS CR
- Tesař V. (2007) *Pressure-Driven Microfluidics*. Artech House Publishers, Boston - London, pp. 389 – 393
- Tesař V. (2008) Valve-Less Rectification Pumps, Chapter in “*Encyclopedia of Microfluidics and Nanofluidics*“, Ed.: Dongqing Li, publ. by Springer Science+Business Media, LLC., ISBN: 978-0-387-48998-8, pp. 2132-2139
- Tesař, V., Jílek, M., Randa, Z. (2001) Topology Changes in an Annular Impinging Jet Flow, *Proc. of Conf. "Topical Problems of Fluid Mechanics 2001"*, p.12, ISBN 80-85918-62-5, Publ. by Inst. of Thermomechanics AS CR, Prague, Czech Republic
- Tesař V., Kordík J. (2009) Quasi-Similarity Model of Synthetic Jets, *Sensors and Actuators A - Physical*, ISSN: 0924-4247, Vol. A 149, p. 255
- Tesař V., Kordík J., Daněk M. (2008) Lift and Separation Control on Wind Turbine Blades by Vortices Having Streamwise Oriented Axes, *Proc. of Colloquium FLUID DYNAMICS 2008*, ISBN 978-80-87012-14-7, publ. by Institute of Thermomechanics AS CR, v.v.i., Prague
- Tesař V., Peszynski K. (2006) Capacitance in Microfluidics, *Pneumatyka*, Nr. 2, 57, p. 29
- Tesař V., Peszynski K. (2009) Annular Synthetic-Jet Actuator for Large Active Distances, *Proc of "ENGINEERING MECHANICS 2009"* Confer. with Internat. Participation, ISBN: 978-80-86246-35-2, p. 1309, Svratka, May 11 – 14
- Tesař V., Trávníček Z. (2005) Pulsating and Synthetic Impinging Jets, *Journal of Visualization*, ISSN 1343-8875, The Visualisation Society of Japan, Vol. 8, No. 3, p. 201
- Tesař V., Trávníček Z. (2006) Apparatus for Collection of Samples from the Surface of Examined Objects, in Czech, *Patent Application* No. PV 2006-214, Patent Office of the Czech Republic
- Tesař V., Trávníček Z. (2008) Excitational Metamorphosis of Surface Flowfield Under an Impinging Annular Jet, *Chemical Engineering Journal*, p. 312, Vol. 144, Issue 2
- Tesař V., Vogel J., Trávníček Z. (2008) Annular Synthetic Jets for Anti-Terrorist Warfare, *Proc. of 12th Intern. Conf. on Developments in Machinery Designs and Control*, publ. by Univ. of Technology and Life Sciences in Bydgoszcz, Poland
- Tesař V., Trávníček Z., Kordík J., Broučková Z. (2009), Fluidic Circuit Theory Applied to Problem of Resonant Frequency of Synthetic-Jet Actuators, *Proc. of 13th International Conference on Developments in Machinery Design and Control*, publ. by Univ. of Technology and Life Sciences in Bydgoszcz, Poland 2009
- Trávníček Z., Tesař V. (2003) Annular Synthetic Jet Used for Impinging Flow Mass Transfer, *International Journal of Heat and Mass Transfer*, Vol. 46, Issue 17, p. 3291